



PCCP

**The Water Trimer Reaction  $\text{OH} + (\text{H}_2\text{O})_3 \rightarrow (\text{H}_2\text{O})_2\text{OH} + \text{H}_2\text{O}$** 

Journal:	<i>Physical Chemistry Chemical Physics</i>
Manuscript ID	CP-ART-03-2020-001418.R1
Article Type:	Paper
Date Submitted by the Author:	17-Apr-2020
Complete List of Authors:	Gao, Aifang; Hebei Key Laboratory of Sustained Utilization and Development of Water Resources,, Li, Guoliang; South China Normal University, School of Chemistry and Environment PENG, BIN; University of Georgia, Computational Chemistry; Center for Computational Quantum Chemistry, MOE Key Laboratory of Theoretical Chemistry of the Environment, South China Normal University Weidman, Jared; University of Georgia, Center for Computational Quantum Chemistry Xie, Yaoming; University of Georgia, Center for Computational Quantum Chemistry Schaefer, Henry; University of Georgia, Computational Chemistry

SCHOLARONE™  
Manuscripts

## The Water Trimer Reaction $\text{OH} + (\text{H}_2\text{O})_3 \rightarrow (\text{H}_2\text{O})_2\text{OH} + \text{H}_2\text{O}$

Aifang Gao,<sup>1,2,4\*</sup> Guoliang Li,<sup>3,4\*</sup> Bin Peng,<sup>3,4</sup>

Jared D. Weidman,<sup>4</sup> Yaoming Xie,<sup>4</sup> and Henry F. Schaefer III<sup>4\*</sup>

<sup>1</sup>*School of Water Resources and Environment, Hebei GEO University,  
Shijiazhuang, 050031, China*

<sup>2</sup>*Hebei Province Collaborative Innovation Center for Sustainable Utilization of Water  
Resources and Optimization of Industrial Structure, Shijiazhuang, 050031, China*

<sup>3</sup>*MOE Key Laboratory of Theoretical Chemistry of the Environment, Center for Computational  
Quantum Chemistry, South China Normal University, Guangzhou 510006, China*

<sup>4</sup>*Center for Computational Quantum Chemistry, University of Georgia,  
Athens, Georgia 30602, U.S.A.*

All important stationary points on the potential energy surface (PES) for the reaction  $\text{OH} + (\text{H}_2\text{O})_3 \rightarrow (\text{H}_2\text{O})_2\text{OH} + \text{H}_2\text{O}$  have been fully optimized using the “gold standard” CCSD(T) method with the large Dunning correlation-consistent cc-pVQZ basis sets. Three types of pathways were found. For the pathway without hydrogen abstraction, the barrier height of the transition state (**TS1**) is predicted to lie 5.9 kcal/mol *below* the reactants. The two major complexes  $(\text{H}_2\text{O})_3 \cdots \text{OH}$  (**CP1** and **CP2a**) are found to lie 6.3 and 11.0 kcal/mol, respectively, *below* the reactants  $[\text{OH} + (\text{H}_2\text{O})_3]$ . For one of the H-abstraction pathways the lowest classical barrier height is predicted to be much higher, 6.1 kcal/mol (**TS2a**) *above* the reactants. For the other H-abstraction pathway the barrier height is even higher, 15.0 (**TS3**) kcal/mol. Vibrational frequencies and the zero-point vibrational energies connected to the PES are also reported. The energy barriers for the H-abstraction pathways are compared with those for the  $\text{OH} + (\text{H}_2\text{O})_2$  and  $\text{OH} + \text{H}_2\text{O}$  reactions, and the effects of the third water on the energetics are usually minor (0.2 kcal/mol).

## Introduction

The hydroxyl radical (OH) is a highly reactive oxidant, which reacts with many types of macromolecules. The OH radical has been found as the most common oxidant in the troposphere, and has a major impact on the pollutants in the Earth's atmosphere.<sup>1</sup> OH has been called as the "atmospheric vacuum cleaner"<sup>2</sup> because of its capacity to remove greenhouse gases, such as NO<sub>2</sub>, CO, SO<sub>2</sub>, O<sub>3</sub>, CH<sub>4</sub>, and hydrochlorofluorocarbons in the atmosphere, and this function is associated to the climate change.<sup>3</sup> The reactive OH radical is also of biological significance, since it may exist in the cell cytoplasm.<sup>4</sup> As it is able to react with most biomolecules including nucleic acids and amino acids, the destructive action of hydroxyl radicals has been implicated in several neurological diseases.<sup>5</sup>

Since many of the above reactions take place in aqueous environments<sup>4,6</sup> and hydration will change the oxidizing capability of the OH radical,<sup>7</sup> the reactions between the OH radical and water clusters are of significance. The increase of the cluster size will help us to understand eventually the interaction between the OH radical and the liquid and solid phases of water. Recently we have reported the potential energy surface (PES) features for the reactions OH + H<sub>2</sub>O and OH + (H<sub>2</sub>O)<sub>2</sub> with the CCSD(T) method.<sup>8,9</sup> However, the hydrogen abstraction reaction for the OH radical with the water trimer has been much less studied. To our knowledge, there is only one theoretical study of some stationary points on the reaction potential surface, based on DFT optimized geometries and the CCSD(T) single-point energies.<sup>10</sup> In the present study we will address the reaction between the hydroxyl radical and the water trimer  $\text{OH} + (\text{H}_2\text{O})_3 \rightarrow (\text{H}_2\text{O})_2\text{OH} + \text{H}_2\text{O}$  adopting CCSD(T) methods to investigate the geometries of all stationary points (including transition states and complexes) and to examine reaction pathways with different energy barriers. Interestingly, Saykally and coworkers found that the water trimer is

apparently the most abundant cluster in pulsed supersonic expansions when the water cluster densities are measured,<sup>11</sup> and this makes the present study of special significance.

The water trimer ( $\text{H}_2\text{O}$ )<sub>3</sub> itself has been studied intensively, both experimentally and theoretically. As early as 1973, Del Bene and Pople predicted the cyclic structure water trimer to have a lower energy than the chain structure with the *ab initio* SCF method.<sup>12</sup> A number of follow up studies confirmed this prediction. The subsequent theoretical works have predicted the stationary-point structures, vibrational frequencies, binding energies, and tunneling motions for the water trimer with various (HF, MP2, and CCSD) methods.<sup>13-22</sup> Experimental studies measured the Vibration-Rotation-Tunneling (VRT) spectra in the gas phase<sup>23-25</sup> and infrared spectra in inert matrices.<sup>26-29</sup> Although much research on the water trimer is not cited here, most of those previous studies have been fortunately summarized by Saykally *et al.*<sup>30</sup> and by Tschumper *et al.*<sup>31</sup> All recent studies concluded that the global minimum for the water trimer is a cyclic six-membered-ring structure with three dangling O-H bonds in the up-up-down positions out of the O<sub>3</sub> plane (denoted as *uud*, the convenient symbol introduced by Schütz *et al.*<sup>15</sup>). Thus, in our present study only the global minimum (*uud* cyclic structure) of the water trimer will be adopted as the reactant in the potential energy surface sketched in Figure 1.

## 1. Theoretical Methods

In the present research, the “gold standard” CCSD(T) method with the cc-pVnZ (n = D, T, Q) basis sets were adopted. The CCSD(T) method denotes the coupled cluster single and double substitutions with a perturbative treatment of triple excitations,<sup>32,33</sup> and cc-pVnZ (n = D, T, Q) denotes the correlation-consistent basis developed by Dunning and co-workers.<sup>34</sup> In the text below, we will simply use DZ, TZ, and QZ to represent these correlation-consistent basis sets.

To ascertain the nature of the stationary points, their harmonic vibrational frequencies were evaluated at the same levels of theory. The CCSD(T) computations with DZ and TZ basis sets were carried out with the CFOUR program,<sup>35</sup> while those with QZ used MOLPRO interfaced with the OPTKING module of Psi4.<sup>36,37</sup>

## 2. Results and Discussion

### 3.1 Outline of Reaction Pathways

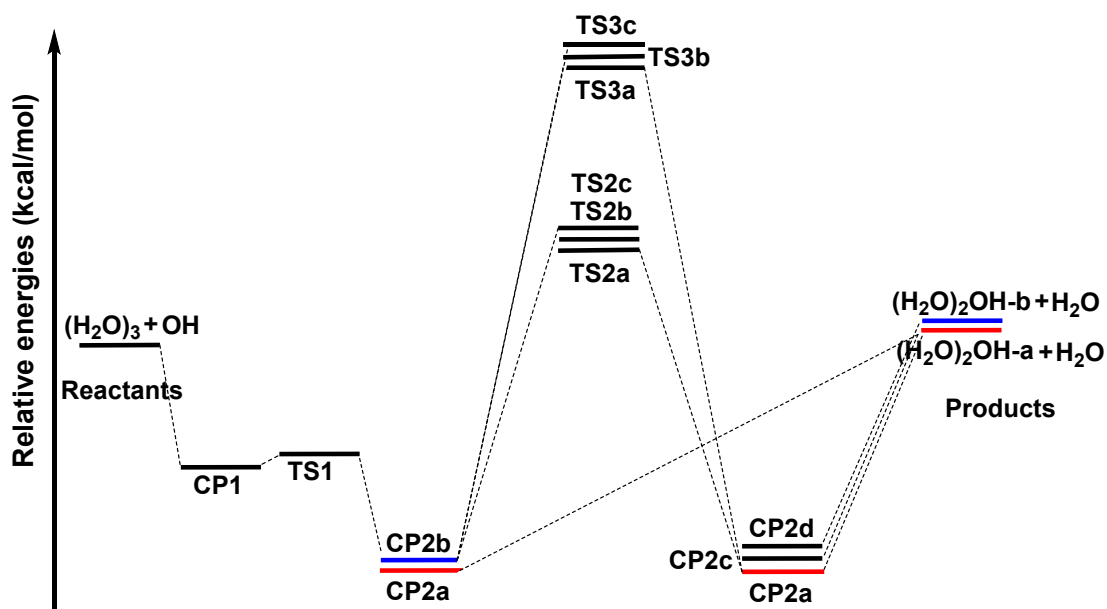


Figure 1. Outline of the various pathways for the  $\text{OH} + (\text{H}_2\text{O})_3$  reaction.

A sketch of the predicted potential energy surface (PES) with the CCSD(T) method for the  $\text{OH} + (\text{H}_2\text{O})_3 \rightarrow (\text{H}_2\text{O})_2\text{-OH} + \text{H}_2\text{O}$  reaction is shown in Figure 1, and the structures of all our stationary points on the potential energy surface are displayed in Figure 2. The sketch of our coupled-cluster PES is (for the most part) qualitatively consistent with the BH&HLYP PES reported by Gonzalez *et al.*<sup>10</sup> Figure 1 shows that the reaction will proceed through two

complexes (**CP1** and **CP2**). A low-barrier transition state (**TS1**) lies between these two complexes. The higher energy barrier transition states (**TS2** and **TS3**) are on the proton transfer pathways between two **CP2** complexes. The details for each pathway on the PES for the  $\text{OH} + (\text{H}_2\text{O})_3 \rightarrow (\text{H}_2\text{O})_2\text{-OH} + \text{H}_2\text{O}$  reaction will be discussed below.

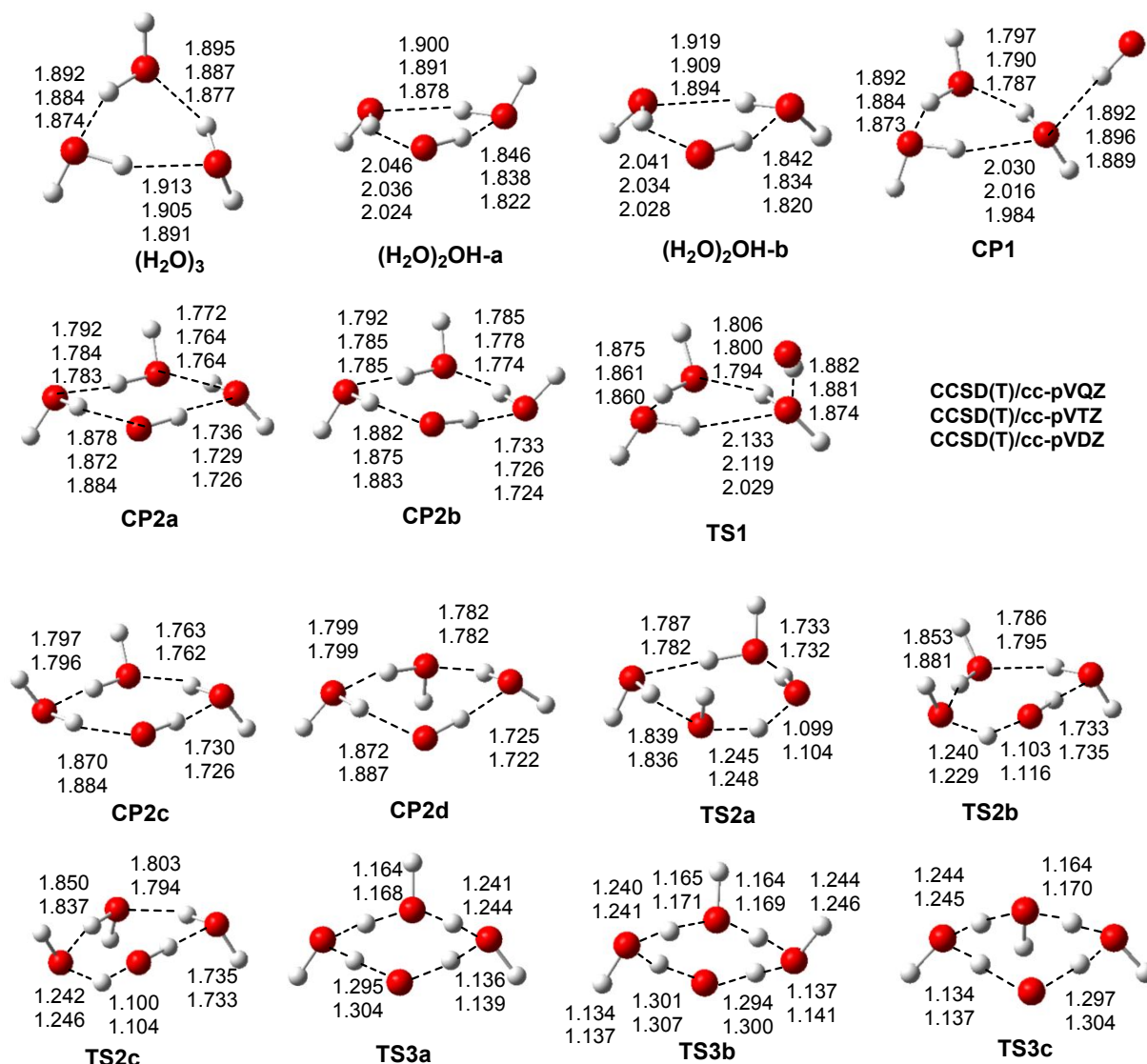


Figure 2. The structures of the complexes and transition states for the  $\text{OH} + (\text{H}_2\text{O})_3$  reaction (distances in Å). The structures in the favorable reaction path (Figure 3) are optimized with the basis sets up to QZ, and those in other paths (Figures 4 and 6) are optimized up to TZ (with QZ single-point energies). The coordinates for all structures are reported in the Supporting Information.

### 3.2. The Low-Barrier Pathway from OH + (H<sub>2</sub>O)<sub>3</sub> to H<sub>2</sub>O + (H<sub>2</sub>O)<sub>2</sub>OH

Figure 3 shows the pathway for the OH + (H<sub>2</sub>O)<sub>3</sub> → H<sub>2</sub>O + (H<sub>2</sub>O)<sub>2</sub>OH reaction by far the lowest energy barrier.

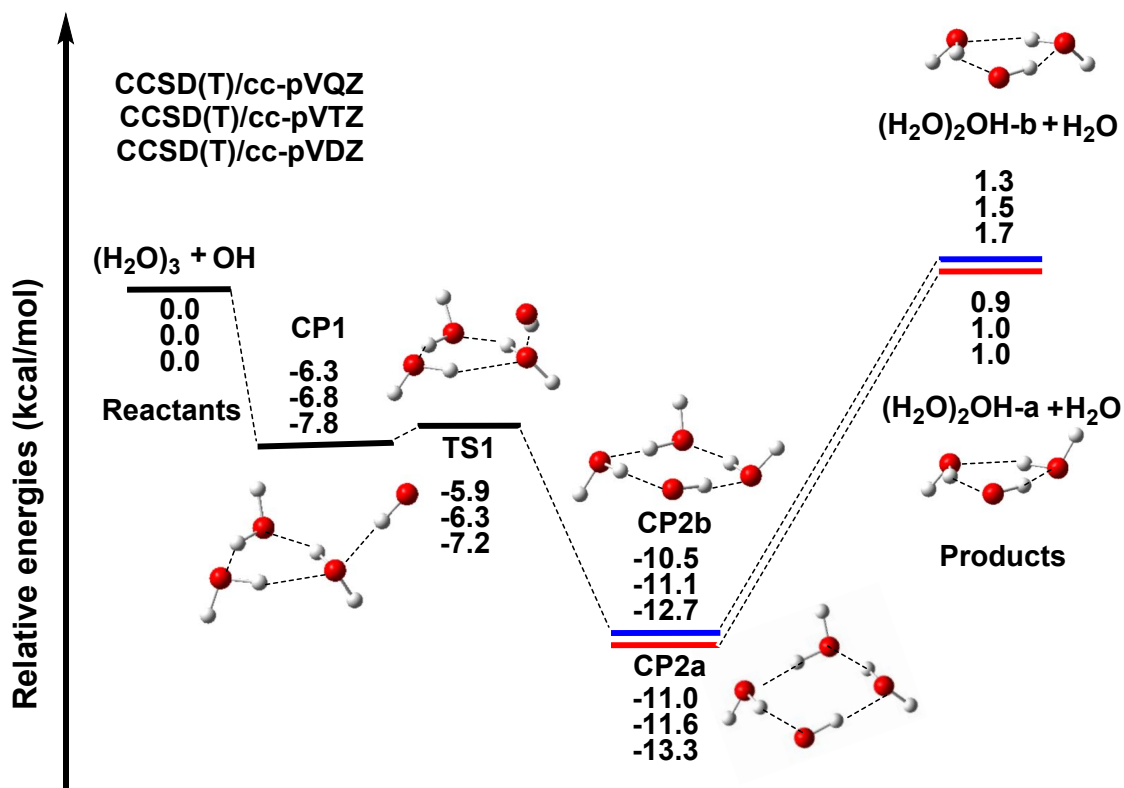


Figure 3. The most favorable pathway for the OH + (H<sub>2</sub>O)<sub>3</sub> → H<sub>2</sub>O + (H<sub>2</sub>O)<sub>2</sub>OH reaction. Note that there are two distinct conformers (**CP2a** and **CP2b**) of the complex (H<sub>2</sub>O)<sub>3</sub>-OH. Relative energies are given in kcal/mol. Every stationary point shown was fully and independently optimized with the CCSD(T) method using all three basis sets.

One of the reactants, the water trimer (H<sub>2</sub>O)<sub>3</sub>, has been studied by many research groups, and various isomers, including first-order and second-order stationary points, have been reported.<sup>16-18</sup> All the recent theoretical studies concluded that the global minimum is the *uud*

cyclic structure.<sup>31</sup> In the present study, our CCSD(T) results confirmed that the *uud*-(H<sub>2</sub>O)<sub>3</sub> conformer is the global minimum (Figure 2), lying lower than the *uuu*-(H<sub>2</sub>O)<sub>3</sub> conformer by 1.0 kcal/mol.<sup>38</sup> Thus, we will use the lowest-lying *uud*-(H<sub>2</sub>O)<sub>3</sub> conformer to study the (H<sub>2</sub>O)<sub>3</sub> plus OH reaction. The three (H<sub>2</sub>O···HOH) hydrogen bonds in the six-membered ring of the cyclic water trimer are similar, 1.895, 1.892, and 1.913 Å predicted by the CCSD(T)/cc-pVQZ method (Figure 2). The three O···O distances ( $r_e$ ) are even more closely related, 2.795, 2.790, and 2.787 Å, respectively, and these results are in agreement with the experimental observation, the average O–O distance ( $r_0$ ) of 2.85 Å.<sup>25</sup>

When the OH radical approaches the water trimer, the entrance complex (H<sub>2</sub>O)<sub>3</sub>···HO (**CP1**) is formed. Structure **CP1** is predicted to lie 6.3 kcal/mol [CCSD(T)/cc-pVQZ] below the separated OH and *uud*-(H<sub>2</sub>O)<sub>3</sub> reactants (Figure 3). **CP1** has a hydrogen bond between the H atom of the OH radical and one of the O atoms in the cyclic water trimer. The new hydrogen bonding O···H distance is predicted to be 1.892 Å at the CCSD(T)/cc-pVQZ level of theory (Figure 2). In this entrance complex **CP1**, the six-membered ring for the water trimer remains, but now the three hydrogen bond distances turn out to be rather different, 1.797, 1.892, and 2.030 Å, respectively (Figure 2). The longest of these (2.030 Å) may be viewed as preliminary to the subsequent OH insertion.

Following the OH···(H<sub>2</sub>O)<sub>3</sub> entrance complex (**CP1**), a transition state (**TS1**) is approached, lying above **CP1** by only 0.4 kcal/mol. Thus, this is an “early” transition state, and its geometry is similar to that of **CP1**. The obvious difference is that the longest hydrogen bond (2.030 Å in **CP1**) becomes even longer (2.133 Å) at **TS1**, further anticipation to OH insertion.

As the OH moiety enters the six-membered ring, the longest hydrogen bond (2.133 Å) is broken, and two new hydrogen bonds are formed, resulting an exit complex **CP2** with an eight-

membered ring, consisting of four O-H bonds and four O $\cdots$ H hydrogen bonds (Figures 2 and 3). There are two distinct (H<sub>2</sub>O)<sub>3</sub>-OH conformers for **CP2**, labelled **CP2a** and **CP2b**, with similar geometries, except for the orientations of the three out-of-plane OH bonds (Figure 2). For **CP2a** the four hydrogen bond distances in the eight-membered ring are 1.736, 1.772, 1.792, and 1.878 Å, respectively, at the CCSD(T)/cc-pVQZ level of theory, and those for **CP2b** are almost the same (within 0.013 Å). In **CP2a** the dangling OH bonds kept their original orientations as in the water trimer, and we can label it as *udu*. (Note: This symbol is the similar to that for water trimer, but the order matters. The symbol here begins with the dangling OH bond closest to the H atom of the OH radical.) For **CP2b**, the directions of the three dangling OH bonds are different, and this structure may be labelled as *uud* (Figure 2). The complex **CP2a** lies 11.0 (QZ), 11.6 kcal/mol (TZ), or 13.3 kcal/mol (DZ) below the reactants, and the complex **CP2b** has slightly higher energy (only 0.5 kcal/mol) than that for **CP2a**.

The previous theoretical studies of the (H<sub>2</sub>O)<sub>3</sub>-OH complex used the MP2 and DFT methods.<sup>39-44</sup> All these studies predicted the same cyclic structure (*udu*) to be the global minimum, and these results are in good agreement with our CCSD(T) predicted structure **CP2a**. To our knowledge, no experimental results are yet available for the (H<sub>2</sub>O)<sub>3</sub>-OH complex, although experimental structures are available for the (H<sub>2</sub>O)-OH and (H<sub>2</sub>O)<sub>2</sub>-OH complexes.<sup>43</sup>

As shown in Figure 3, the complexes **CP2a** or **CP2b** can dissociate directly into the reaction products, H<sub>2</sub>O + (H<sub>2</sub>O)<sub>2</sub>OH, without a transition state. In this procedure, a H<sub>2</sub>O molecule separates itself from the eight-membered ring, and the remaining part (H<sub>2</sub>O)<sub>2</sub>OH forms a six-membered ring, composed of three O-H covalent bonds and three O $\cdots$ H hydrogen bonds (Figures 2 and 3). There are two different (H<sub>2</sub>O)<sub>2</sub>OH conformers, (H<sub>2</sub>O)<sub>2</sub>OH-**a** and (H<sub>2</sub>O)<sub>2</sub>OH-**b**,

corresponding to the **CP2a** or **CP2b** complexes, respectively. The energy difference between  $(\text{H}_2\text{O})_2\text{OH-a}$  and  $(\text{H}_2\text{O})_2\text{OH-b}$  is small, namely 0.4 kcal/mol with the QZ basis sets. The lowest-lying products,  $(\text{H}_2\text{O})_2\text{OH-a}$  plus  $\text{H}_2\text{O}$ , lie above the reactants by 0.9 kcal/mol (QZ) or 1.0 kcal/mol (TZ and DZ). The ZPVE corrected reaction enthalpy will be even smaller (see Section 3.5).

### 3.3. Hydrogen Abstraction via Transition State TS2

In the pathway described in the previous section, there is no energy barrier. This is because there is only hydrogen bond cleavage, instead of H-abstraction. In other words, there is no O-H covalent bond broken in that pathway. In this section, we will consider the pathways containing hydrogen-transfer (H-abstraction) between two different **CP2** conformers (Figure 4). Since the O-H bond cleavage is involved in these pathways, significant energy barriers are inevitable.

The first kind of the hydrogen abstraction pathway is via transition state **TS2** (Figure 1). From the complex **CP2a**, a H atom in a water molecule (the out-of-plane H atom linked to atom  $\text{O}_2$  in Figure 5) shifts to the oxygen atom ( $\text{O}_1$ ) of the hydroxyl radical moiety to lead to **TS2a**. The geometry of **TS2a** involves an eight-membered ring, with the shifted H atom located between the O atoms ( $\text{O}_1$  and  $\text{O}_2$ ). The distances of the two hydrogen bonds, i.e.,  $\text{O}_1 \cdots \text{H}$  and  $\text{H} \cdots \text{O}_2$  in **TS2a**, are predicted with the TZ basis set to be  $\sim 1.25 \text{ \AA}$  and  $\sim 1.10 \text{ \AA}$ , respectively (Figure 2). When the shifted H atom in **TS2a** further moves to the oxygen atom ( $\text{O}_1$ ) to form a new H- $\text{O}_1$  covalent bond, the other hydrogen atom adjacent to atom  $\text{O}_1$  simultaneously protrudes out of the ring plane, resulting in another **CP2a** complex (the right side in Figure 4). Figure 5 displays the **CP2a**  $\rightarrow$  **TS2a**  $\rightarrow$  **CP2a** connection, and the two **CP2a** structures before and after

**TS2a** are mirror images. Structure **TS2a** is predicted to lie above the reactants OH + (H<sub>2</sub>O)<sub>3</sub> by 6.1 (QZ single-point energy), 5.5 (TZ) or 5.2 (DZ) kcal/mol.

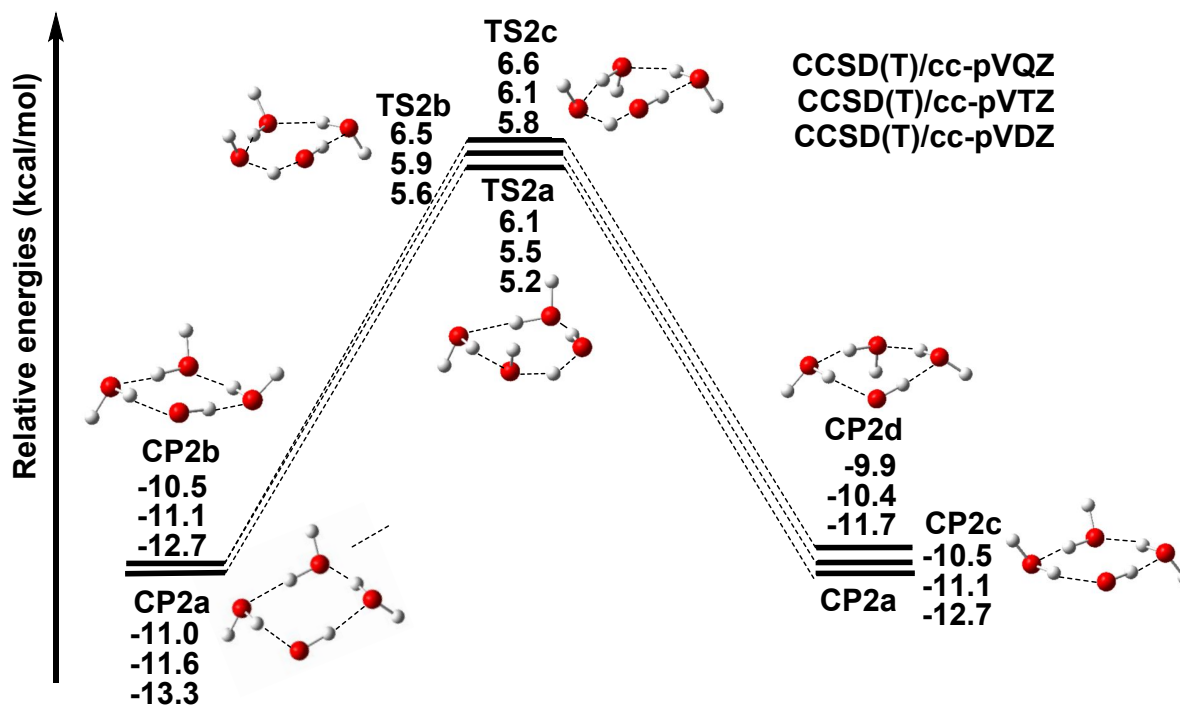


Figure 4. Sketch of the PES for the H-abstraction pathway between different conformers of the **CP2** complex via the transition state **TS2**. The QZ energies are the single-point energies at the TZ optimization geometries.

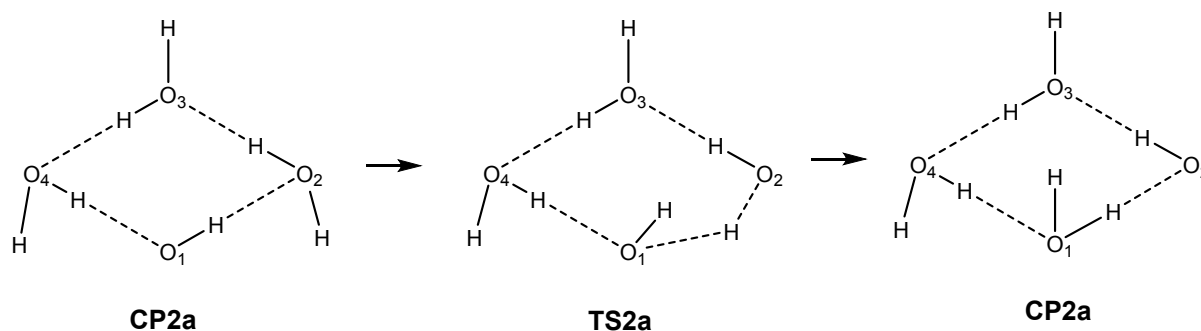


Figure 5. The H-abstraction reaction within **CP2a** via the transition state **TS2**. Note that the two **CP2a** structures before and after **TS2a** are mirror images.

There are other two conformers for **TS2**. In addition to **TS2a**, which is a *udu* conformer, the other conformers **TS2b** and **TS2c** each displays three dangling H atoms in the “up-down-down” (*udd*) position and in the “up-up-down” (*uud*) positions, respectively. Structures **TS2b** and **TS2c** lie slightly higher than **TS2a**, by 0.4 and 0.5 kcal/mol, respectively. The conformer **TS2b** connects to the **CP2b** and **CP2c** complexes, where **CP2b** is a *uud* conformer and **CP2c** is a *udd* conformer (Figures 2 and 4). The transition state **TS2c** connects the **CP2b** and **CP2d** complexes, where **CP2d** is a *uuu* conformer (Figures 2 and 4).

### 3.4. Reaction via **TS3**

A different kind of hydrogen abstraction pathway goes through the transition state **TS3** ( $C_s$  symmetry, Figure 6). Distinct from the pathways involving **TS2**, in the **TS3** pathway all four H atoms in the eight-membered ring are moving simultaneously. In the eight-membered ring skeleton of **TS3** all eight O $\cdots$ H distances are in the range from  $\sim 1.14$  to  $\sim 1.30$  Å (Figure 2), which are much shorter than a typical O $\cdots$ H hydrogen bond ( $\sim 1.9$  Å), but longer than a conventional O-H bond ( $\sim 0.96$  Å). Figure 6 shows that the lowest conformer **TS3a**, labelled as *udu* (i.e., up-down-up) based on the three out-of-plane O-H orientations, lies above the reactants, OH + (H<sub>2</sub>O)<sub>3</sub>, by 15.0 (QZ), 13.5 (TZ), and 12.4 (DZ) kcal/mol, which is much higher than **TS2**. The large energy barrier for **TS3** is not surprising, since four O-H bonds are broken at the same time. Like the **TS2a** pathway, the **TS3a** pathway is symmetrical, each side connecting a **CP2a** structure (Figure 6). The predicted larger energy barrier for the **TS3** pathway suggests that it plays little role in the atmospheric chemistry.

There are two other conformers **TS3b** (*uud*) and **TS3c** (*uuu*), based on the out-of-plane O-H orientations, and both lie slightly above **TS3a**, within 2.0 kcal/mol (QZ). **TS3b** connects **CP2b** and **CP2c**, while **TS3c** connects two **CP2d** structures.

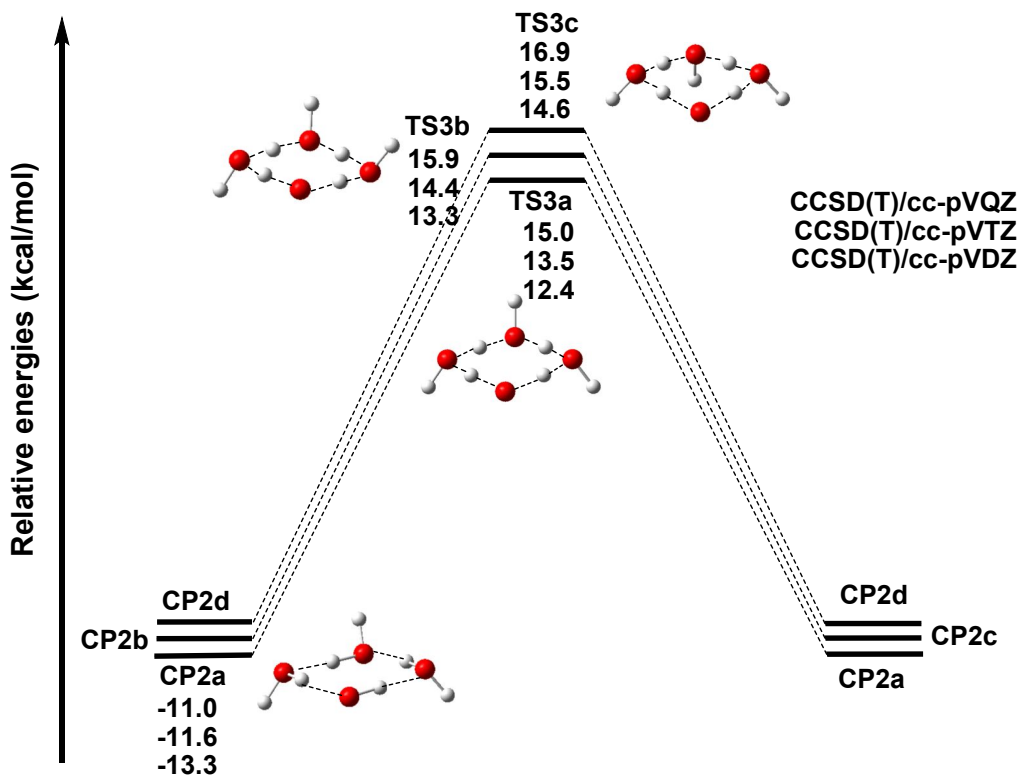


Figure 6. The pathway via transition state **TS3**, in which four hydrogen atoms are moving simultaneously. The QZ energies are the single-point energies at the TZ optimization geometries.

Table 1. Harmonic vibrational frequencies (in  $\text{cm}^{-1}$ ) and zero-point vibrational energies (ZPVE, in kcal/mol) for the stationary points of the  $\text{OH} + (\text{H}_2\text{O})_3 \rightarrow (\text{H}_2\text{O})_2\text{-OH} + \text{H}_2\text{O}$  reaction. The CCSD(T) method was used with two correlation consistent Dunning basis sets. The quantity  $\Delta\text{ZPVE}$  is the change in energy due to ZPVE relative to the separated reactants  $(\text{H}_2\text{O})_3 + \text{OH}$ .

	$\Delta\text{E}$	ZPVE	$\Delta\text{ZPVE}$	$\Delta\text{E}_{\text{ZPVE}}$	Harmonic vibrational frequencies
<b>cc-pVDZ</b>					
$(\text{H}_2\text{O})_3 + \text{OH}$	0.0	52.2	0.0	0.0	3881,3878,3877,3684,3681,3599,1736,1724,1716,974,701,651,505,413,391,271,242,232,221,209,203 ( $\text{H}_2\text{O})_3$ ; 3703 (OH)
<b>CP1</b>	-7.8	54.1	1.9	-5.9	3889,3876,3873,3734,3662,3630,3517,1726,1716,1706,1001,770,663,602,515,492,413,380,283,274,268,234,205,201,167,32,18
<b>CP2a</b>	-13.3	54.7	2.5	-10.8	3883,3879,3875,3668,3601,3530,3349,1740,1726,1705,1038,870,822,714,622,470,445,359,318,289,270,256,246,229,207,77,45
<b>TS1</b>	-7.2	53.7	1.6	-5.6	3893,3892,3876,3756,3661,3645,3543,1723,1719,1704,962,748,638,563,497,458,414,330,290,263,237,212,197,185,153,27,47i
<b>TS2a</b>	5.2	51.9	-0.3	4.9	3876,3873,3779,3648,3573,3368,1780,1730,1724,1517,1084,922,845,732,670,489,457,453,330,289,279,256,242,220,112,54,1904i
<b>TS3a</b>	12.4	49.3	-2.9	9.5	3850,3850,3846,1851,1826,1717,1677,1646,1587,1523,1388,1368,1265,1140,732,685,666,608,580,558,554,545,409,394,134,74,1629i
$(\text{H}_2\text{O})_2\text{OH-a} + \text{H}_2\text{O}$	1.0	51.8	-0.4	0.6	3886,3880,3735,3664,3466,1716,1695,952,701,629,575,416,301,283,248,230,209,181 [ $(\text{H}_2\text{O})_2\text{OH}$ ]; 3928,3822,1690 ( $\text{H}_2\text{O}$ )
<b>cc-pVTZ</b>					
$(\text{H}_2\text{O})_3 + \text{OH}$	0.0	51.8	0.0	0.0	3909,3907,3903,3689,3683,3613,1707,1690,1685,926,689,614,471,372,360,253,228,209,202,194,188 ( $\text{H}_2\text{O})_3$ ; 3745 (OH)
<b>CP1</b>	-6.8	53.6	1.8	-5.0	3915,3899,3898,3746,3673,3630,3526,1701,1682,1677,955,746,640,565,479,455,378,360,274,262,256,216,186,182,162,30,15
<b>CP2a</b>	-11.6	54.2	2.3	-9.3	3907,3905,3900,3651,3589,3522,3359,1715,1696,1681,996,841,798,658,590,451,425,356,294,274,254,245,234,215,200,79,45
<b>TS1</b>	-6.3	53.1	1.3	-5.0	3926,3911,3902,3781,3679,3638,3560,1708,1686,1672,902,708,621,531,429,414,360,324,266,254,224,199,182,142,85,37,39i
<b>TS2a</b>	5.5	51.4	-0.4	5.1	3901,3899,3804,3639,3569,3362,1741,1702,1690,1491,1067,713,659,473,436,432,308,281,264,241,228,210,109,52,1845i
<b>TS3a</b>	13.5	49.0	-2.8	10.7	3888,3888,3876,1868,1779,1692,1636,1598,1565,1505,1331,1323,1214,1102,733,683,668,620,593,559,551,538,420,407,146,77,1614i
$(\text{H}_2\text{O})_2\text{OH-a} + \text{H}_2\text{O}$	1.0	51.4	-0.4	0.6	3911,3908,3737,3675,3498,1687,1667,916,668,557,534,375,291,252,230,211,196,163 [ $(\text{H}_2\text{O})_2\text{OH}$ ]; 3946,3841,1669 ( $\text{H}_2\text{O}$ )

### 3.5. Vibrational Frequencies and Zero-Point Vibrational Energies

Table 1 reports the harmonic vibrational frequencies for the stationary points (the lowest conformer of each) of the  $\text{OH} + (\text{H}_2\text{O})_3$  reaction predicted with the CCSD(T) method with both DZ and TZ basis sets. Table 1 shows that the transition states (**TS1**, **TS2a**, **TS3a**) for the three

pathways have imaginary vibrational frequencies of  $47i$ ,  $1904i$ , and  $1629i$   $\text{cm}^{-1}$  (DZ) or  $39i$ ,  $1845i$ , and  $1614i$   $\text{cm}^{-1}$  (TZ), respectively. Note that the magnitude of the imaginary frequency for **TS1** is very small, since the very flat PES around **TS1** is related to the similar geometries and close energies (difference of 0.5 kcal/mol) between **TS1** and **CP1** (Figure 3).

Table 1 also shows the zero-point vibrational energies (ZPVEs), and the ZPVE values can be used to correct the relative energies for all the stationary points. At the CCSD(T)/TZ level of theory, the reaction enthalpy is reduced from 1.0 kcal/mol ( $\Delta E$ , in Table 1) to 0.6 kcal/mol ( $\Delta E_{\text{ZPVE}}$ ) after the ZPVE correction. The energy barriers of **TS1**, **TS2a**, and **TS3a** are changed by the ZPVE corrections from -6.3, 5.5, and 13.5 kcal/mol ( $\Delta E$ , in Table 1) to -5.0, 5.1, and 10.7 kcal/mol ( $\Delta E_{\text{ZPVE}}$ ), respectively. We may also approximately apply the TZ ZPVE corrections to the QZ energies. Therefore, the most reliable (QZ energies with the TZ ZPVE corrections) results are 0.5 kcal/mol for reaction enthalpy, -4.5, 5.7, and 12.2 kcal/mol for the **TS1**, **TS2a**, and **TS3a** barrier, respectively.

### 3.6. Comparisons with $\text{OH} + (\text{H}_2\text{O})_2$ and $\text{OH} + \text{H}_2\text{O}$

Previous research<sup>8,9</sup> examined the hydrogen abstraction reaction from water monomer to the OH radical ( $\text{OH} + \text{H}_2\text{O} \rightarrow \text{H}_2\text{O} + \text{OH}$ ) and that from water dimer to the OH radical [ $\text{OH} + (\text{H}_2\text{O})_2 \rightarrow (\text{H}_2\text{O})\text{-OH} + \text{H}_2\text{O}$ ]. Figure 7 shows the comparison of the three H-abstraction reactions. All three reactions are based on results from the same CCSD(T)/cc-pVQZ level of theory, (single-point energies at the TZ geometries for **TS2a** of trimer + OH).

The monomer complex,  $\text{H}_2\text{O}\cdots\text{OH}$  (**CP1**)<sup>9</sup>, is predicted to lie 6.1 kcal/mol below the reactants at the CCSD(T)/cc-pVQZ level of theory, the corresponding binding energies for the

dimer complex and the trimer complex are predicted to be 10.8 kcal/mol (the entrance complex **CPa**)<sup>8</sup> and 11.0 kcal/mol (the entrance complex **CP2a**), respectively. The second water increases the  $\text{H}_2\text{O}\cdots\text{OH}$  dissociation energy by about 4.7 kcal/mol. This is mainly caused by the formation of the second  $\text{O}\cdots\text{H}$  hydrogen bond. The effect of the third water on the energetics is minor (0.2 kcal/mol) compared with the dimer reaction, because there is no further hydrogen bond formed involving the third water molecule.

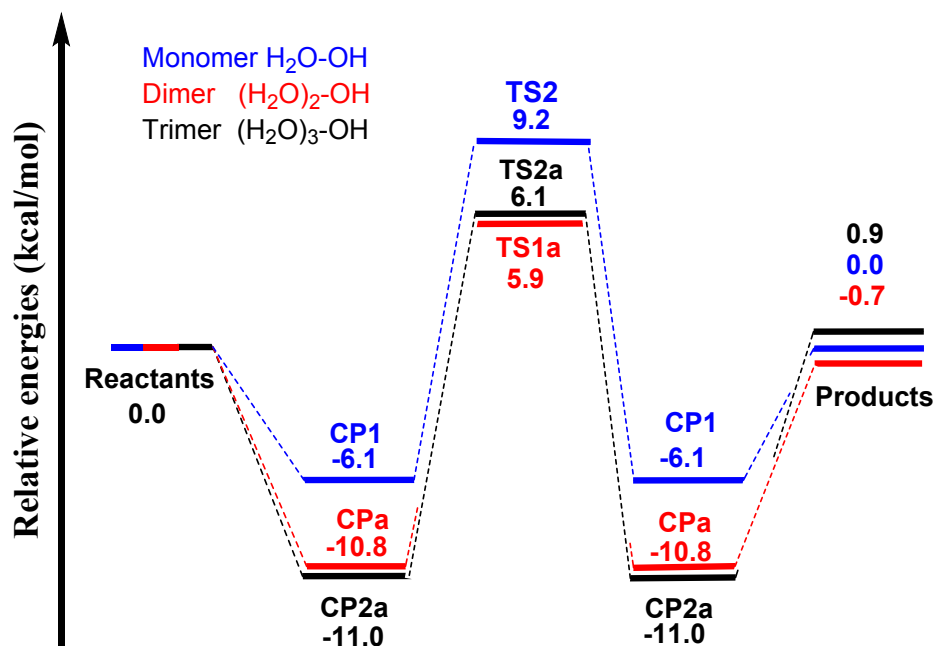


Figure 7. Comparison the potential energy surface for the hydrogen abstraction  $\text{OH} + (\text{H}_2\text{O})_3$  reaction (black) with those of the  $\text{OH} + (\text{H}_2\text{O})_2$  (red)<sup>8</sup> and the  $\text{OH} + \text{H}_2\text{O}$  (blue)<sup>9</sup> reactions at the CCSD(T)/cc-pVQZ level of theory. (For **TS2a** of the trimer + OH reaction, single-point energies are used).

From the same reason, the second water molecule lowers the energy barrier for the H-abstraction reaction from 9.2 kcal/mol (**TS1** for the water monomer reaction) to 5.9 kcal/mol (**TS1a** for water dimer reaction).<sup>8,9</sup> However, the third water does not further lower the energy

barrier, which is predicted to be 6.1 kcal/mol (**TS2a** in the present study). Since the energy barrier difference from dimer to trimer has converged within 0.2 kcal/mol, it is reasonably expected that for the tetramer and higher-order polymers the further change will be comparable.

The water monomer  $\text{OH} + \text{H}_2\text{O} \rightarrow \text{H}_2\text{O} + \text{OH}$  reaction is a symmetric reaction, because the products are the same as the reactants, and the reaction energy is absolutely zero. Though the H-abstraction reactions for the water dimer and the water trimer are not symmetrical, the reaction energies are still small (-0.7 kcal/mol for  $\text{OH} + (\text{H}_2\text{O})_2$  and +0.9 kcal/mol for  $\text{OH} + (\text{H}_2\text{O})_3$  at the level of CCSD(T)/cc-pVQZ). This is due to the fact that the same bonds are present for both sides of the reaction. For the reaction of water dimer with the OH radical  $[\text{OH} + (\text{H}_2\text{O})_2 \rightarrow (\text{H}_2\text{O})\text{-OH} + \text{H}_2\text{O}]$ , there is one hydrogen bond for both reactants and products. For the reaction of water trimer with the OH radical  $[\text{OH} + (\text{H}_2\text{O})_3 \rightarrow (\text{H}_2\text{O})_2\text{-OH} + \text{H}_2\text{O}]$ , there are three hydrogen bonds for both reactants and products. Thus, for all these reactions, the energy differences between the reactants and products should be small, and the reaction energies of -0.7 and +0.9 kcal/mol are fairly reasonable.

## Conclusions

The water trimer reaction  $\text{OH} + (\text{H}_2\text{O})_3 \rightarrow (\text{H}_2\text{O}_2\text{-OH} + \text{H}_2\text{O})$  has been investigated using the “Gold Standard” CCSD(T) method along with basis sets up to cc-pVQZ. We choose the global minimum of the water trimer *uud*-( $\text{H}_2\text{O}$ )<sub>3</sub> as the reactant. There are three classes of pathways for this reaction, and we predicted several features for these pathways.

1. All the pathways go through the complex (**CP1**), the transition state (**TS1**), and eight-membered ring complex (**CP2**).

2. The complex **CP2** has four cyclic conformers, based on the relative orientations of the three out-of-plane hydrogen atoms. These conformers are nearly degenerate (within 1.2 kcal/mol, TZ), with the *udu* form lying the lowest.

3. The first pathway has a low energy barrier (**TS1**), since only hydrogen bonds are broken. It is actually a procedure that involves a H<sub>2</sub>O moiety in the water trimer replaced by the OH radical without hydrogen abstraction. Note that the transition state **TS1** lies only 0.5 kcal/mol above the **CP1** complex, and still 5.9 kcal/mol below the reactants.

4. For a hydrogen abstraction pathway over the **TS2a** transition state, a hydrogen atom moves from the water trimer to the OH radical. In other words, the OH radical moiety in the **CP2** complex captures a hydrogen atom and leaves a (H<sub>2</sub>O)<sub>2</sub>OH complex. The energy barrier is predicted to be higher (6.1 kcal/mol, CCSD(T)/cc-pVQZ), since this pathway involves the breakage of a conventional O-H bond.

5. Another hydrogen abstraction pathway over the **TS3** transition state has an even higher energy barrier (15.0 kcal/mol, CCSD(T)/cc-pVQZ). In this mechanism, four O-H bonds in the eight-membered ring are broken simultaneously.

6. In previous research<sup>9</sup> concerning H atom abstraction from the water dimer, it was found that the second water molecule, like a catalyst, reduces the barrier from 9.2 kcal/mol for the water monomer reaction to 6.1 kcal/mol (Figure 7). This is because there is one more hydrogen bond formed in the transition state for the water dimer reaction. However, we found in this research that the third water molecule only slightly (0.2 kcal/mol) reduce the barrier, because there is no further hydrogen bond formed in the transition state with the third water molecule.

7. The “Gold Standard” CCSD(T) method is necessary for accurate predictions for the title reaction. One should be cautious to use low-level (such as DFT) theoretical methods, since these methods may predict the energy barriers in a wide range.<sup>45</sup>

8. We are hopeful that this research will assist in the experimental observation of the  $(\text{H}_2\text{O})_3\text{-OH}$  radical.

### **Conflicts of interest**

There are no conflicts of interest to declare.

### **ACKNOWLEDGMENTS**

This work was supported by the Scientific Pre-Research Fund of Hebei GEO University in 2015(YK201501), the Young Talent Plan of Hebei Province in China. Research at the University of Georgia was supported by the U.S. Department of Energy, Office of Basic Energy Sciences, Theoretical and Computational Chemistry (CTC) Program, Grant DE-SC0018412. We thank Dr. J. M. Anglada for providing details of their results.<sup>10</sup>

## REFERENCES

---

- 1 I. S. A. Isaksen and S. B. Dalsøren, *Science*, 2011, **331**, 38-39.
- 2 T. E. Graedel, *Chemical Compounds in the Atmosphere* (Academic Press, New York), 1978, p. 375-376.
- 3 J. H. Seinfeld and S. N. Pandis, *Atmospheric Chemistry and Physics: From Air Pollution to Climate Change*, 1st ed. (John Wiley & Sons: New York), 1998.
- 4 R. J. Reiter, D. Melchiorri, E. Sewerynek, B. Poeggeler, L. Barlow-Walden, J. Chuang, G. G. Ortiz and D. Acuña-Castroviejo, *J. Pineal. Res.*, 1995, **18**, 1-11.
- 5 W. Linert, G. N. L. Jameson and *J. Inorg. Biochem.*, 2000, **79**, 319-326.
- 6 W. L. Chameides and D. D. Davis, *J. Geophys. Res.: Oceans.*, 1982, **87**, 4863-4877.
- 7 S. Du, J. S. Francisco, G. K. Schenter, T. D. Iordanov, B. C. Garret, M. Dupuis and J. Li, *J. Chem. Phys.*, 2006, **124**, 224318.
- 8 A. Gao, G. Li, B. Peng, Y. Xie and H. F. Schaefer, *J. Phys. Chem. A*, 2016, **120**, 10223-10230.
- 9 A. Gao, G. Li, B. Peng, Y. Xie and H. F. Schaefer, *Phys. Chem. Chem. Phys.*, 2017, **19**, 18279-18287.
- 10 J. Gonzalez, M. Caballero, A. Aguilar-Mogas, M. Torrent-Sucarrat, R. Crehuet, A. Solé, X. Giménez, S. Olivella, J. M. Bofill and J. M. Anglada, *Theor. Chem. Acc.*, 2011, **128**, 579-592.
- 11 J. B. Paul, C. P. Collier, R. J. Saykally, J. J. Scherer and A. O'Keefe, *J. Phys. Chem. A*, 1997, **101**, 5211-5214.
- 12 J. E. Del Bene and J. A. Pople, *J. Chem. Phys.*, 1973, **58**, 3605-3608.
- 13 H. Kistenmacher, G. C. Lie, H. Popkie and E. Clementi, *J. Chem. Phys.*, 1974, **61**, 546-561.
- 14 E. Honegger and S. Leutwyler, *J. Chem. Phys.*, 1988, **88**, 2582-2595.
- 15 M. Schütz, T. Bürgi, S. Leutwyler and H. B. Bürgi, *J. Chem. Phys.*, 1993, **99**, 5228-5238.
- 16 S. S. Xantheas and T. H. Dunning, *J. Chem. Phys.*, 1993, **98**, 8037-8040.
- 17 J. E. Fowler and H. F. Schaefer, *J. Am. Chem. Soc.*, 1995, **117**, 446-452.
- 18 W. Klopper, M. Schütz, H. P. Lüthi and S. Leutwyler, *J. Chem. Phys.*, 1995, **103**, 1085-1098.
- 19 J. A. Anderson, K. Crager, L. Fedoroff and G. S. Tschumper, *J. Chem. Phys.*, 2004, **121**, 11023-11029.

- 
- 20 T. Salmi, H. G. Kjaergaard and L. Halonen, *J. Phys. Chem. A*, 2009, **113**, 9124-9132.
- 21 L. C. Ch'ng, A. K. Samanta, Y. Wang, J. M. Bowman and H. Reisler, *J. Phys. Chem. A*, 2013, **117**, 7207-7216.
- 22 E. Miliordos, E. Aprà and S. S. Xantheas, *J. Chem. Phys.*, 2013, **139**, 114302.
- 23 N. Pugliano and R. J. Saykally, *Science*, 1992, **257**, 1937-1940.
- 24 K. Liu, M. J. Elrod, J. G. Loeser, J. D. Cruzan, N. Pugliano, M. G. Brown, J. Rzepiela and R. J. Saykally, *Faraday Discuss.*, 1994, **97**, 35-41.
- 25 F. N. Keutsch and R. J. Saykally, *PNAS*, 2001, **98**, 10533-10540.
- 26 A. Engdahl and B. Nelander, *J. Chem. Phys.*, 1987, **86**, 4831-4837.
- 27 J. Ceponkus, G. Karlstrom and B. Nelander, *J. Phys. Chem. A*, 2005, **109**, 7859-7864.
- 28 B. Tremblay, B. Madebène, M. E. Alikhani and J. P. Perchard, *Chem. Phys.*, 2010, **378**, 27-36.
- 29 J. Ceponkus, A. Engdahl, P. Uvdal and B. Nelander, *Chem. Phys. Lett.*, 2013, **581**, 1-9.
- 30 F. N. Keutsch, J. D. Cruzan and R. J. Saykally, *Chem. Rev.*, 2003, **103**, 2533-2578.
- 31 J. C. Howard and G. S. Tschumper, *WIREs: Comput. Mol. Sci.*, 2014, **4**, 199-224.
- 32 G. D. Purvis and R. J. Bartlett, *J. Chem. Phys.*, 1982, **76**, 1910-1918.
- 33 K. Raghavachari, G. W. Trucks, J. A. Pople and M. Head-Gordon, *Chem. Phys. Lett.*, 1989, **157**, 479-483.
- 34 T. H. Dunning, *J. Chem. Phys.*, 1989, **90**, 1007-1023.
- 35 CFOUR, a quantum chemical program package written by: J. F. Stanton, J. Gauss, M. E. Harding, P. G. Szalay, with contributions from: A. A. Auer, R. J. Bartlett, U. Benedikt, C. Berger, D. E. Bernholdt, Y. J. Bomble, L. Cheng, O. Christiansen, M. Heckert, O. Heun, C. Huber, T.-C. Jagau, D. Jonsson, J. Jusélius, K. Klein, W. J. Lauderdale, D. A. Matthews, T. Metzroth, D. P. O'Neill, D. R. Price, E. Prochnow, K. Ruud, F. Schiffmann, W. Schwalbach, S. Stopkowicz, A. Tajti, J. Vázquez, F. Wang, J. D. Watts, and the integral packages MOLECULE (J. Almlöf and P. R. Taylor), PROPS (P. R. Taylor), ABACUS (T. Helgaker, H. J. A. Jensen, P. Jørgensen and J. Olsen), and ECP routines by A. V. Mitin and C. van Wüllen, 2010.

- 
- 36 MOLPRO, version 2012.1, a Package of *ab initio* Programs, H.-J. Werner, P. J. Knowles, G. Knizia, F. R. Manby, M. Schütz, P. Celani, W. Györffy, D. Kats, T. Korona, R. Lindh, A. Mitrushenkov, G. Rauhut, K. R. Shamasundar, T. B. Adler, R. D. Amos, S. J. Bennie, A. Bernhardsson, A. Berning, D. L. Cooper, M. J. O. Deegan, A. J. Dobbyn, F. Eckert, E. Goll, C. Hampel, A. Hesselmann, G. Hetzer, T. Hrenar, G. Jansen, C. Köppl, S. J. R. Lee, Y. Liu, A. W. Lloyd, Q. Ma, R. A. Mata, A. J. May, S. J. McNicholas, W. Meyer, T. F. {Miller III}, M. E. Mura, A. Nicklaß, D. P. O'Neill, P. Palmieri, D. Peng, K. Pflüger, R. Pitzer, M. Reiher, T. Shiozaki, H. Stoll, A. J. Stone, R. Tarroni, T. Thorsteinsson, M. Wang and M. Welborn, see <http://www.molpro.net>, 2012.
- 37 R. M. Parrish, L. A. Burns, D. G. A. Smith, A. C. Simmonett, A. E. DePrince, E. G. Hohenstein, U. Bozkaya, A. Y. Sokolov, R. Di Remigio, R. M. Richard, J. F. Gonthier, A. M. James, H. R. McAlexander, A. A. Kumar, M. Saitow, X. Wang, B. P. Pritchard, P. Verma, H. F. Patkowski, K. King, R. A. Valeev, E. F. Evangelista, F. A. Turney, J. M. Schaefer, T. D. Crawford and C. D. Sherrill, *J. Chem. Theory Comput.*, 2017, **13**, 3185-3197.
- 38 G. Li, Q.-S. Li, Y. Xie and H. F. Schaefer, *Angew. Chem.*, 2015, **127**, 11375-11378.
- 39 S. Hamad, S. Lago and J. A. Mejías, *J. Phys. Chem. A*, 2002, **106**, 9104-9113.
- 40 P. C. do Couto, R. C. Guedes, B. J. C. Cabral and J. A. M. Simões, *J. Chem. Phys.*, 2003, **119**, 7344-7355.
- 41 X. L. Dong, Z. Y. Zhou, L. J. Tian and G. Zhao, *Int. J. Quant. Chem.*, 2005, **102**, 461-469.
- 42 M. A. Allodi, M. E. Dunn, J. Livada, K. N. Kirschner and G. C. Shields, *J. Phys. Chem. A*, 2006, **110**, 13283-13289.
- 43 K. Tsuji and K. Shibuya, *J. Phys. Chem. A*, 2009, **113**, 9945-9951.
- 44 F. J. J. Hernandez, T. Brice, C. M. Leavitt, T. Liang, P. L. Raston, G. A. Pino and G. E. Douberly, *J. Chem. Phys.*, 2015, **143**, 164304.
- 45 G. Li, L. Zhou, Q.-S. Li, Y. Xie and H. F. Schaefer, *Phys. Chem. Chem. Phys.*, 2012, **14**, 10891-10895.